FLOW OF λ-DNA IN MICROFLUIDIC DEVICES

Polly J. Shrewsbury (1), Susan J. Muller (2), Dorian Liepmann (3)

(1) Bioengineering Program, Berkeley Sensor and Actuator Center, University of California Berkeley, Berkeley, CA 94720, USA –Tel +1 510 642 3699, Email pollys@socrates.berkeley.edu
(2) Department of Chemical Engineering, University of California Berkeley, Berkeley, CA 94720, USA –Tel +1 510 642 4525, Email muller2@socrates.berkeley.edu
(3) Department of Bioengineering, Berkeley Sensor and Actuator Center, University of California Berkeley, Berkeley, CA 94720, USA –Tel +1 510 642 9360, Email liepmann@me.berkeley.edu

***Abstract* – This research seeks to understand the behavior of biological macromolecules in microfluidic devices. Epifluorescence microscopy was used to observe the conformation of λ-DNA macromolecules during flow through sudden expansions, sudden contractions, straight channels, and a valve. Our analysis indicates that both the flow patterns within the device and the device geometry can influence macromolecular structure and stability. Utilization of this type of analysis in the design of microsystems for biochemical processing is instrumental for maintaining molecular stability and for ensuring accuracy of sample analysis.**

I. INTRODUCTION

Inherent in microfluidic systems is the potential for parallel processing and high throughput analyses, improved sensitivity in particle detection, process automation, and increased cost efficiency. Already researchers have demonstrated use of microsystems for performing multiple biochemical protocols including capillary electrophoresis, cell fractionation, DNA sequencing, electrochromatography, and polymerase chain reaction (PCR) [1]. A complementary area of research is the design and fabrication of components intended to facilitate these processes [2,3]. The intent of this work is to bridge the gap between these two areas of research and to focus on the behavior of biological macromolecules flowing through microfluidic devices. Of particular interest is the effect of flow and device geometry on macromolecular transport and conformation. Correlating microfluidic parameters and device geometries with macromolecular behavior enables improvements in the design and efficiency of micro total analysis systems intended for biochemical processing. Accordingly, the flow of λ-DNA solutions having varying concentrations and viscosities has been studied through geometries likely to comprise an actual microsystem: straight channels, sudden contractions, sudden expansions, and a micro check valve.

II. MATERIALS AND METHODS

The straight channel microfluidic device and the planar micro check valve were fabricated from silicon. Photolithography techniques were employed to transfer patterns from masks to the wafer surface. Using either thermally grown oxide or photoresist as a masking layer, a reactive ion etch (RIE) allowed definition of device feature depth. To enclose the fluidic path following fabrication, epoxy was used to bond a thin coverglass ($t < 170$ μm) to the surface of the device. Polyvinyl tubing was then affixed to through-holes located in device reservoirs to enable the mechanical control of fluid flow via a syringe pump. A more inclusive description of the fabrication process for the microfluidic straight channel device appears in Shrewsbury, et al. [4], and that for the micro check valve appears in Deshmuck, et al [5].

Epifluorescence microscopy was used to visualize λ-DNA molecules. The molecules were labeled with the fluorescent dye YOYO-1 at a base pair:dye ratio of 5:1. In all experiments, λ-DNA was diluted to the specified concentration in a buffer solution containing 10 mM tris-HCl, 2 mM EDTA, 10 mM NaCl, and 4% β-mercaptoethanol. Bulk solution viscosities were increased as noted using sucrose. An Olympus IX70 inverted epifluorescence microscope equipped with a mercury burner served as the illumination source. A fluorescence cube having the following optical characteristics was used with the probe YOYO-1: excitation 460–500 nm, long pass beamsplitter 505 nm, emission 510-560 nm. The microscope was coupled to a Videoscope International high-gain image intensifier and a Cohu high performance monochrome CCD camera. All data were recorded to video. The data were transferred to a Macintosh G3 and analyzed using a Scion framegrabber and NIH Image software.

III. CHARACTERIZATION OF STRAIGHT CHANNEL MICROFLUIDIC DEVICE

The scanning electron micrograph in Fig. 1 illustrates the geometry of the microfluidic channel. The channel is 300 μm wide (in z), 60 μm deep (in y), and 8000 μm long (in x). Both ends of the channel terminate at two identical reservoirs. Fluid enters and exits the device by passing through holes located in these reservoirs. An important feature of the device is the narrowing of the fluidic path from the reservoir into the channel. This contraction produces an elongational flow. From equations for

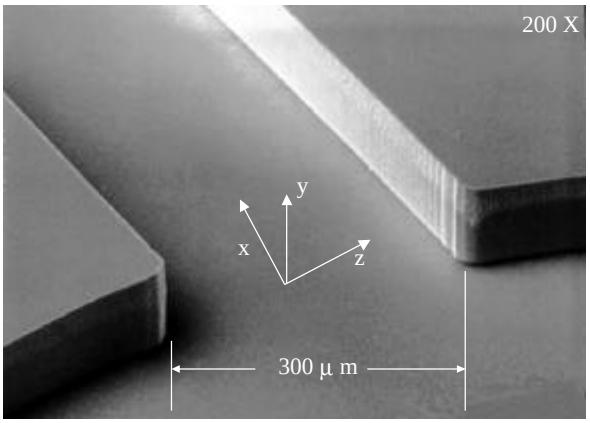

Fig. 1: SEM of Microfluidic Channel

Newtonian fluid flow through a rectangular geometry, the elongational flow (and the extension rate) is highest along the centerline of the channel. In contrast, the shear flow dominates at channel walls and surfaces.

IV. FLOW OF λ-DNA IN MICROFLUIDIC CHANNEL

In a first experiment to understand how macromolecules behave in a microfluidic flow, a 0.3 μg/ml solution of λ-DNA molecules was visualized at 100X magnification flowing through the center of a microfluidic channel. In order to avoid entrance effects, the imaging location was placed downstream of the channel entrance, at a distance approximately equal to 1/3 the total channel length. Two solution viscosities (η = 1 cpoise, 25 cpoise) were studied at three flow rates (10 μl/hr, 20 μl/hr, 30 μl/hr). Fluorescent beads were imaged under identical experimental conditions to verify the absence of optical artifacts, stemming from limitations in the camera capture rate, in the recorded images. Sample λ-DNA images from the experiment for η = 25 cpoise appear in Fig. 2. Also shown are the maximum Deborah numbers (De) for the given set of experimental conditions. Here,

$$De = \gamma\lambda \qquad (1)$$

where γ is the shear rate at the wall and λ is the relaxation time of λ-DNA molecules, as experimentally determined from rheological measurements (see Shrewsbury et al. for details).

The λ-DNA molecules in the 1 cpoise solution (not shown) seemingly elongate along streamlines at increasing flow rates and De numbers. A comparison of these images to beads, however, reveals that optical streaking obscures any stretching, as the beads mirror the pattern of the DNA. Thus, to continue pursuing this method of investigation, the solution viscosity, in lieu of shear rate, was increased in order to impose greater stress on the molecules but without altering the flow rate.

As reflected in Fig. 2, the conformational changes in the λ-DNA for the 25 cpoise solution were striking. Increasing the solvent viscosity increased the relaxation time of the molecule, and dramatic changes in

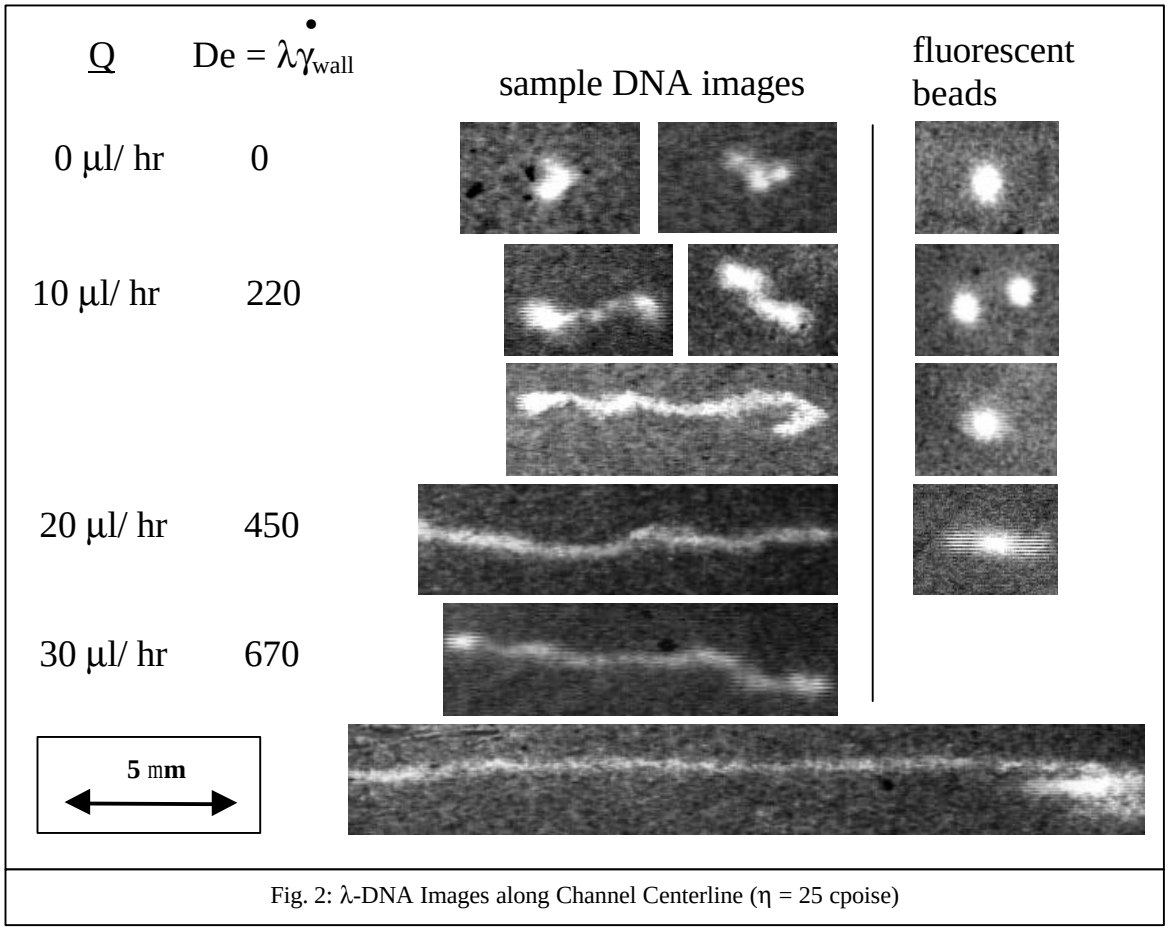

Fig. 2: λ-DNA Images along Channel Centerline (η = 25 cpoise)

conformation could be observed at flow rates where streaking is negligible. Compare, for example, the images in Fig. 2 of the beads and of the DNA at a flow rate of 20 µl/hr. A histogram analysis recording the length distribution of a minimum of 100 molecules at each flow rate was conducted. The analysis (histograms not shown) indicates that a broad range of molecular conformations exists at all flow rates, and that molecular stretching is non-monotonic with flow rate.

The molecular deformation observed may be attributable to a combination of an elongational and a shear flow. At the channel centerline, the shear rates should be extremely low and, at the imaging location, the elongation channel entrance effects should have partially dissipated. Thus, two experiments to elucidate the relative contribution of each flow type to the observed effects logically follow. The first experiment examines an elongational flow along the channel centerline, and the second explores the shear flow at the channel wall.

V. λ-DNA IN ELONGATIONAL FLOW

An elongational flow exists at the channel centerline; the fluid accelerates as it enters the channel from the upstream reservoir and decelerates as it exits the channel into the downstream reservoir. Therefore, imaging DNA molecules moving through the centerline of the device lends insight into the impact of a converging and diverging flow in molecular conformation and identifies the positions within the device most likely to produce deformation of molecules. By using the fine focus of the microscope to locate the top and then bottom of the device (approximately 0.6 µm/division), the channel centerline was found. As illustrated in Fig. 3, the imaging position varied along x, the direction of flow, while the y and z positions remained constant. The concentration of DNA in buffered solution was 0.3 µg/ml, the viscosity was 15 centipoise, and the flow rate was 5 µl/hr.

At **A**, the DNA molecule is in the device reservoir. The shape, as represented by the representative sample images in Fig. 3, is coiled. Having fully entered the channel at **B** and having just undergone a converging flow, the DNA molecules are highly elongated. Dividing flow rate by the device cross-sectional area gives a mean fluid velocity of 0.077 mm/s within the channel. In this 15 centipoise viscosity solution, the relaxation time of the molecule is 0.682 s. Therefore, in traveling 0.053 mm along the centerline, only about one relaxation time will have elapsed, and a significant fraction of the elongational stress from entering the channel will not yet have relaxed. At position **C**, the approximate midpoint of the 8 mm channel, the DNA molecules as seen in the sample images are still not entirely relaxed. Greater relaxation of the molecule is observed further downstream of the channel entrance, at positions **D** and **E**. Not until the molecule exits the channel at **F**, however, does the molecule recover the conformation observed at **A**.

A histogram analysis tracking the length distribution of a minimum of 100 molecules at each position (not shown) supports the above qualitative findings. As seen in the sample images in Fig. 3, the DNA molecules elongate in the extensional flow at **B**. Only after exiting the channel at **F** do the molecules return to a relaxed, coiled conformation observed in the device entrance reservoir at **A**. As previously, fluorescent beads were imaged under identical flow conditions experienced by DNA molecules to ensure optical streaking did not bias the measurements.

This experiment demonstrates that an elongational

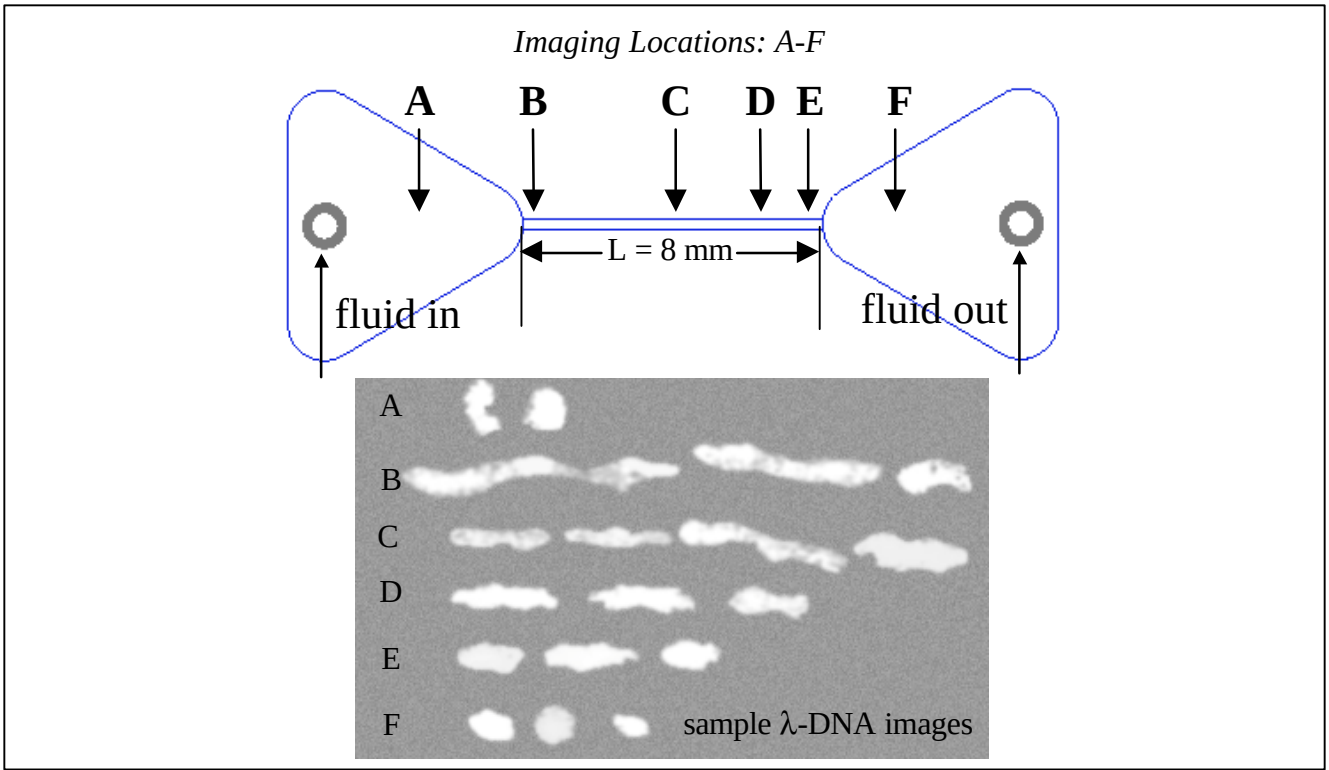

Fig. 3: λ-DNA in Elongational Flow

flow in a microfluidic device can cause DNA molecules to stretch, and that the time required for the molecules to recover their initial conformation exceeds the relaxation time by a large factor. The data suggests that an understanding of the fluid relaxation time and the detailed kinematics is critical when designing microfluidic devices. Without this knowledge, the placement of too many stresses in series will stretch and degrade the molecules and will bias any analysis.

VI. λ-DNA IN SHEAR FLOW

To address the impact of shear flow on molecular conformation, DNA molecules were imaged at 100X magnification at 3 locations within the channel. Fig. 4 depicts these imaging positions. The "upstream" wall location immediately follows the channel entrance, and the "downstream" location precedes the channel exit. At the channel wall upstream, the channel wall downstream, and the channel centerline, images were recorded at 5 depths (in z): at 6 μm, 12 μm, 30 μm, 48 μm, and 54 μm from the top channel surface. The total channel depth was 60 μm. The top and bottom of the channel were located as previously described. In these experiments the DNA concentration was 0.3 μg/ml, the solution viscosity was 42 cpoise, and the flow rate was 5 μl/hr.

Analogous to the analysis for the elongational flow, the lengths of a minimum of 100 molecules were measured at each depth. Table 1 contains a summary of the means, medians, and standard deviations of the data. As previously, fluorescent beads were measured to ensure optical streaking did not bias the measured lengths of molecules.

As discussed, the shear rate is highest near the top and bottom walls and approaches zero at the channel midplane (y=30 μm). This is reflected in increased stretching of the molecules near the top and bottom of the channel, and relatively little stretching, and a much narrower distribution of conformations, near the midplane. Any residual deformation of the molecules due to the elongational flow associated with the contraction flow is modest relative to the deformation induced by shear at the walls. Theoretically, the shear rate at equal distances from

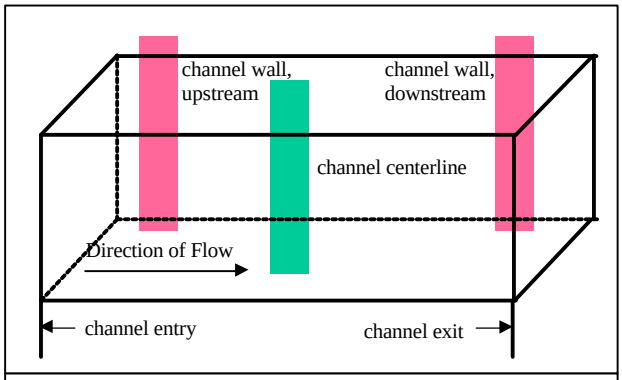

Fig. 4: Imaging Positions in Microchannel

the channel midplane is identical. Therefore, the distribution of molecular lengths at 6 μm and 12 μm should mirror that at 54 μm and 48 μm, respectively. Differences may arise from dissimilar surfaces at the channel top (glass) and channel bottom (silicon) or from the limited sample size (>100 molecules per depth).

At the upstream wall location, the proximity to the top and bottom surfaces results in a shear rate that is highest at these surfaces and decreases – but remains high – near the channel midplane. The data means (and histograms) at all vertical locations are much more similar than those means for the data recorded at the upstream center location. In particular, comparison of upstream wall data to the upstream center data reveals that the molecules are much more stretched near the midplane of the channel at the wall location than close to the centerline. Comparison of the two locations at y =30 μm is perhaps the most compelling: at the channel center the histogram (not shown) is very narrow and the mean length is 1.5 μm; at the wall a much broader spectrum of lengths is observed and the mean length is 1.8 μm.

An examination of the upstream wall data to the downstream wall data reveals a disparity between the distributions of DNA lengths at corresponding depths near the wall, but at different axial positions within the channel. At the downstream wall position, the data means are essentially similar at all vertical positions within the channel; an analysis of molecular distribution indicates that the population of longer molecules is smaller. In fact,

Table 1: Mean and Median Lengths for Dilute Solutions of λ-DNA

depth, μm	upstream wall	upstream center	downstream wall
6 μm	mean: 3.6 ± 2.1 μm median: 3.0 μm	mean: 3.6 ± 2.4 μm median: 3.0 μm	mean: 2.5 ± 1.5 μm median: 1.8 μm
12 μm	mean: 3.2 ± 2.1 μm median: 2.4 μm	mean: 3.6 ± 2.5 μm median: 2.9 μm	mean: 2.8 ± 2.1 μm median: 1.9 μm
30 μm	mean: 2.4 ± 1.4 μm median: 1.8 μm	mean: 1.7 ± 0.8 μm median: 1.5 μm	mean: 2.6 ± 1.7 μm median: 1.8 μm
48 μm	mean: 2.9 ± 1.8 μm median: 2.4 μm	mean: 1.9 ± 0.8 μm median: 1.7 μm	mean: 2.9 ± 2.1 μm median: 1.8 μm
54 μm	mean: 3.1 ± 1.8 μm median: 2.4 μm	mean: 3.7 ± 2.6 μm median: 2.8 μm	mean: 2.3 ± 1.8 μm median: 1.7 μm

at the positions nearest to the top and bottom walls, the mean DNA length has dropped from 3 and 2.4 μm upstream to 1.8 and 1.7 μm at the downstream location. The decrease in mean length with axial distance suggests that the DNA is undergoing chain scission in this high shear flow, and that the molecules are being irreversibly degraded. This hypothesis is currently under study in our laboratory.

VII. CONCENTRATION EFFECTS

In an actual microsystem, the concentration of macromolecules in solution will vary depending upon the composition of the test sample and on the processing stage. For viscoelastic polymers such as DNA, the properties of the bulk solution are dependent upon concentration. Therefore, in order to adapt a conventional laboratory protocol to the microscale an understanding of this dependence, and of any manifestations of it in terms of solution behavior, is critical. Accordingly, we extended our previous analysis to more concentrated solutions of λ-DNA molecules.

Using an identical microfluidic straight channel device and operating under identical flow conditions, we repeated our previous experiments but increased the solution concentration of λ-DNA to 28.15 μg/ml. At this concentration, c = 0.1c*, where c* is the overlap concentration. Of the total DNA in solution, only 0.15 μg/ml received a fluorescent label. Labeling this fraction of molecules avoids excess fluorescence which obscured visualization.

As for the experiments in dilute solution, the molecules were imaged at the same 3 locations within the channel (upstream wall, upstream center, and downstream wall) and at 3 depths (6 μm, 30 μm, 54 μm). A summary of the mean and median molecular lengths for this data appears in Table 2. Referring to Table 2, the mean and median molecular lengths at all depths are similar. This similarity is striking and contrasts with that observed for λ-DNA molecules in dilute solution. As reflected in Table 1, at the same imaging positions and flow conditions, molecules in dilute solution exhibit a more pronounced change in length with channel depth due to varying shear rate.

The most pronounced similarity between the dilute solution data and the concentrated solution data is the decreased molecular length at the channel centerline (i.e., upstream center, depth of 30 μm). In both cases, the mean and median lengths of molecules are smaller at this depth than at other depths. At this position, the shear is identically zero. All other depths and imaging locations experience some shear flow. Therefore, this data suggests that while the molecules response to shear flow or mixed shear and extension is sensitive to concentration, its response to the elongational flow along the centerline is relatively insensitive to concentration changes over this range (i.e., up to 0.1c*).

An interesting dissimilarity exists between the dilute and the concentrated solution data on molecular conformation at the upstream wall location and the downstream wall location. As delineated in Table 1, the mean molecular lengths of molecules in dilute solution decrease when traveling from the upstream wall to the downstream wall location, suggesting that a high De flow can induce irreversible molecular damage through chain scission of molecules.

For the same De flow, this behavior, however, seems not to hold for the concentrated case. In Table 2, the mean and median molecular lengths are similar at all downstream wall locations, and resemble closely the mean and median molecular lengths recorded at the upstream wall locations. Here again, the dynamics of molecular interactions in concentrated solution differ from those in dilute solution. This observed change in behavior can only stem from the increased concentration of macromolecules in solution. The implication is that the greater number of molecules in solution act in a manner that more effectively dissipates an applied stress than dilute solutions of molecules.

VIII. DNA LADENED FLUID IN A MICROCHECK VALVE

In an attempt to examine the extent to which device geometry and flow effects the conformation of macromolecules in a real, microfluidic device, λ-DNA was imaged in flow in a micro check valve. The device is

Table 2: Mean and Median Lengths for More Concentrated Solutions of λ-DNA

depth, μm	upstream wall	upstream center	downstream wall
6 μm	mean: 2.5 ± 1.4 μm median: 2.1 μm	mean: 3.3 ± 2.0 μm median: 2.9 μm	mean: 2.5 ± 1.4 μm median: 2.1 μm
30 μm	mean: 3.0 ± 1.9 μm median: 2.2 μm	mean: 1.7 ± 0.4 μm median: 1.6 μm	mean: 2.4 ± 1.6 μm median: 2.0 μm
54 μm	mean: 2.7 ± 1.5 μm median: 2.2 μm	mean: 3.0 ± 1.5 μm median: 2.5 μm	mean: 2.1 ± 1.3 μm median: 1.8 μm

shown in Fig. 5. Flow in the direction indicated moves the central element to the 'open' position, and fluid can travel along the circuitous path on either side of the central, symmetrical axis of the device. Here, the more convoluted fluid path leads to a much more complex flow field than in the straight channels.

As in the preceding experiments, representative molecules are shown at seven locations downstream of the

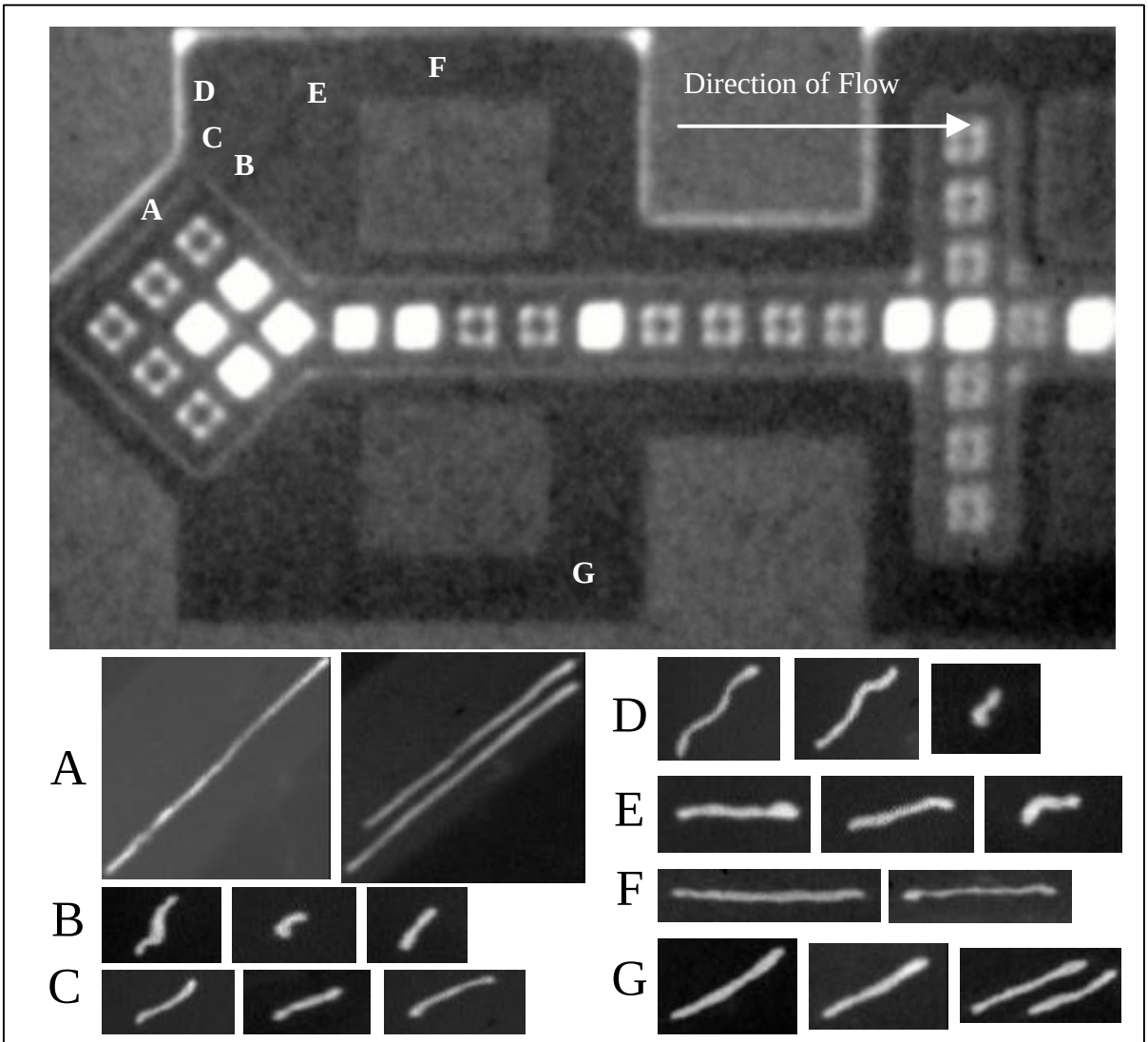

Fig. 5: λ-DNA Flow through Microcheck Valve

entrance, marked A through G in Fig. 5. The images reveal the dramatic changes in both molecule length and orientation due to the flow. As in the straight channel experiments depicted in Fig. 3, such changes in conformation are likely to persist well downstream of the region of the flow which causes them.

IX. CONCLUSIONS

The conformation of λ-DNA in both the relatively simple flow into and along a straight channel and in the complex flow in a micro check valve has been quantified using epifluorescence microscopy. In the former flow, both elongation and shear flow resulted in dramatic stretching of the molecules. The elongational flow along the channel centerline caused remarkably persistent changes in the molecule length: once stretched, the DNA was slow to relax back to the coiled state. In the high shear rate flow near the channel walls, these preliminary studies suggest that irreversible chain scission may be occurring. Visualization in the micro check valve suggests the importance of these effects in real devices. Both conformational changes and chain scission will affect the response of the macromolecules to local sensors or processing steps, and warrant further study.

ACKNOWLEDGMENTS

This work was supported by DARPA though the Composite CAD program managed by Dr. Anantha Krishnan and the microFLUME program managed by Dr. Abe Lee.

REFERENCES

[1] P. Simpson, et al. (1998) *Proc. Natl. Acad. Sci.* **95**, 2256-2261.
[2] P. Graveson, J. Branebjerg, O. Jensen (1993) *J. Micromech. Microeng.* **3**, 168-182.
[3] C. Ho, Y. Tai (1998) *Annu. Rev. Fluid Mech.* **30**, 579-612.
[4] P.J. Shrewsbury, S.J. Muller, D. Liepmann (2000) submitted *Physics of Fluids*.
[5] A. Deshmukh, D. Liepmann, A.P. Pisano (2000) *IEEE Workshop on Solid-State Sensor & Actuator Workshop, Hilton Head, SC.*